Spin-spin relaxation and multiple echoes in manganese ferrites

J. H. Davis and C. W. Searle
Department of Physics, University of Manitoba, Winnipeg, Manitoba, Canada
(Received 30 April 1973)

The Suhl-Nakamura or indirect spin-spin interaction is found to be the predominant relaxation mechanism for manganese nuclei on the A sites in manganese ferrites at temperatures below 4.2 °K. The relaxation time of the first spin echo has been measured at $T = 1.5$ and 4.2 °K as a function of frequency and applied field. The results are compared to the predictions of the calculated Suhl-Nakamara relaxation rate assuming an inhomogeneously broadened resonance line. The amplitude of the first echo is calculated using the density-matrix approach and it is shown that the first echo, via the Suhl-Nakamura interaction, acts as an effective third rf pulse which causes the refocusing of the spin system resulting in the observed second and third echoes. The relaxation times of these additional echoes are calculated and compared with the observed values.

1. INTRODUCTION

Whenever an ordered magnetic insulator contains a high concentration of identical nuclear spins, the indirect spin-spin interaction, introduced to the literature by Suhl[1] and Nakamura,[2] is expected to play a large role in the nuclear magnetic relaxation at low temperatures. The observation of frequency pulling[3] in the Mn^{55} nuclear resonance in Mn^{2+} ions on $MnFe_2O_4$ A sites suggested the possibility of an appreciable spin-spin coupling in this material. As reported earlier,[4] the occurrence of a large number of spin echoes following a two-pulse excitation was observed and may be a direct result of the Suhl-Nakamura interaction between the manganese nuclei.

The A-site Mn^{55} nuclear resonance has a half-width at half-maximum of ~3 MHz, independent of temperature (from 77 to 4.2 °K) while, for example, at 4.2 °K the spin-echo decay time is ~20 μsec, implying that the line is inhomogeneously broadened. Spin-echo measurements are then very useful in the study of the low-temperature relaxation in this system.

The frequency and field dependence of the amplitude and relaxation time of the first echo show that the Suhl-Nakamura interaction is responsible for a large part of the spin-spin relaxation in this material. The frequency dependence of the relaxation time (Fig. 3) gives an especially striking illustration of this effect. The T_2 measurements of Petrov and Petrov[5] will be seen to be in substantial agreement with those reported here. The temperature dependence of T_2 which they reported is suggested to be due to spin-wave processes and the absence of the field dependence of T_2 in their data is likely due to the incomplete saturation of their sample by the external fields (up to ~6 kOe) which they used.

By a density-matrix treatment, the second echo is shown to be stimulated by the formation of the first echo. As evidence it is seen that the amplitude of the first echo is proportional to the square of the enhancement factor ($A_1 \propto \eta^2$) as expected, while the second echo's amplitude is seen to vary as η^3. Further, the field and frequency dependences of the relaxation time are calculated and compare favorably with experiment.

Some experimental results of measurements of relaxation times for the third echo are also discussed. In this case the analysis is felt to be incomplete in that contributions to the third echo due to the refocusing effects of the second echo have not been included.

These results indicate that the occurrence of large numbers of spin echoes following a two-pulse excitation is quite straightforward when there exists a nuclear spin-spin coupling such as that provided by the Suhl-Nakamura interaction.

The present discussion then is largely concerned with the field dependence of the resonance and relaxation of manganese nuclei on the tetrahedral or A sites in manganese ferrite. The experimental work was performed primarily at 4.2 and 1.5 °K in external fields from 0 to 10 kOe using a variable-frequency incoherent-pulse spectrometer. The relaxation times were determined by comparing the echo envelope to an exponential curve of known time constant. The error bars on the experimental values for the relaxation times represent a probable error of 10% in all cases.

Section II contains a general discussion of the resonance condition and frequency pulling while Sec. III discusses contributions to the relaxation, especially the Suhl-Nakamura interaction, and compares the results of some approximate calculations to the experimentally observed field and frequency dependence of the nuclear relaxation. Section IV describes how the Suhl-Nakamura interaction can result in a refocusing of the nuclear magnetization to yield multiple echoes and the discus-

sion of Sec. III is extended to describe the relaxation of the second and third echoes. Finally, Sec. V briefly concludes the discussion.

II. NUCLEAR RESONANCE AND FREQUENCY PULLING IN MANGANESE FERRITE

Stoichiometric manganese ferrite has the spinel structure with formula unit[6] $Mn^{2+}_{0.8}Fe^{3+}_{0.2}[Mn^{3+}_{0.2}Fe^{3+}_{1.6}Fe^{2+}_{0.2}]O_4$, where the cations outside the brackets occupy the tetrahedral or A sites and the cations inside the brackets occupy the octahedral or B sites. From magnetization measurements it was determined that the single crystal of $Ni_{0.03}Mn_{0.62}Fe_{2.36}O_4$ used in these experiments has a moment of $4.54\mu_B$ per formula unit. The approximate formula unit for this crystal is $Mn^{2+}_{0.355}Fe^{3+}_{0.645}[Mn^{3+}_{0.265}Fe^{3+}_{1.06}Fe^{2+}_{0.645}Ni^{2+}_{0.03}]O_4$, assuming the nickel present is Ni^{2+} on the B sites. The nuclear resonance at 586 MHz in manganese ferrite is that of the nuclei in Mn^{2+} ions on the A sites.

The resonance condition is obtained from the coupled equations of motion

$$\frac{d\vec{M}_A}{dt} = \gamma_e [\vec{M}_A \times (\vec{H} - \lambda \vec{M}_B + \vec{H}_A - \alpha \vec{m})] ,$$

$$\frac{d\vec{M}_B}{dt} = \gamma_e [\vec{M}_B \times (\vec{H} - \lambda \vec{M}_A + \vec{H}_B)] ,$$

$$\frac{d\vec{m}}{dt} = \gamma_N [\vec{m} \times (\vec{H} - \alpha \vec{M}_A)] ,$$

where $\vec{M}_A$ and $\vec{M}_B$ are, respectively, the A- and B-site electronic sublattice magnetizations, and $\vec{m}$ is the A-site nuclear magnetization. [The B-site nuclear magnetization is ignored here since, due to the large difference (~100 kOe) in the hyperfine fields of the manganese nuclei on the different sites,[7] the intersublattice nuclei are expected to be effectively uncoupled. Further, the effect on nuclei on the A sites due to disturbances in the electronic magnetization caused by nuclei on the B sites is expected to be quite small.] Here $\vec{H}$ is an applied magnetic field, $\vec{H}_A$ and $\vec{H}_B$ are effective fields describing the anisotropy on the A and B sites, λ is the molecular field constant, and $\alpha = |H_N/M_A^0|$, where $H_N = 559.5$ kOe is the A-site Mn^{2+} hyperfine field at $T = 4.2$ °K, while M_A^0, M_B^0, and m^0 are the z components of the appropriate magnetizations. Finally, $\gamma_e = 2\pi \times 2.8 \times 10^6$ $(\text{sec Oe})^{-1}$ and $\gamma_N = 2\pi \times 1.055 \times 10^3$ $(\text{sec Oe})^{-1}$ are the electronic and Mn^{55}-nuclear gyromagnetic ratios. If the magnetizations are assumed to vary harmonically in time with frequency ω, $M(t) = M^0 e^{-i\omega t}$, taking $M^+ = M^x + iM^y$ the equations for M_A^+, M_B^+, and m^+ are

$$(\omega/\gamma_e) M_A^+ - (H - \lambda M_B^0 - H_A - \alpha m^0) M_A^+ - \lambda M_B^+ M_A^0 - \alpha m^+ M_A^0 = 0 , \quad (1a)$$

$$(\omega/\gamma_e) M_B^+ - (H + \lambda M_A^0 + H_B) M_B^+ + \lambda M_B^0 M_A^+ = 0, \quad (1b)$$

$$(\omega/\gamma_N) m^+ - (H + \alpha M_A^0) m^+ + \alpha m^0 M_A^+ = 0 . \quad (1c)$$

The low-frequency solution of Eqs. (1a)-(1c) represents the nuclear resonance frequency, thus, ignoring terms like (ω/γ_e) which are small for low frequencies, the resonance condition is written as

$$\omega = \gamma_N (H_0 - H_D) + \gamma_N H_N [1 - \eta (m^0/M_A^0)] , \quad (2)$$

where the enhancement factor η is

$$\eta = H_N / [(H_0 - H_D)(\beta - 1) + (\beta H_B + H_A) + \alpha m^0] ,$$

where now H in Eqs. (1) has been replaced by $H_0 - H_D$ where H_0 is the externally applied field, and H_D is the demagnetizing field of the single-crystal sample. The ratio of z components of sublattice magnetizations β is determined by noting that $M_T = M_B - M_A = 4.54\mu_B$, and $M_A = 5.0\mu_B$, thus $\beta = M_B/M_A = 1.9$.

In manganese ferrite, nuclei in domains as well as those in domain walls participate in the resonance.[3,8] For nuclei in domains the enhancement factor, with $T = 1.5$ °K, $H_K = \beta H_B + H_A = 0.6$ kOe, $H_0 - H_D = 0$, and $\beta = 1.9$, is $\eta \simeq 1000$.

Thus, a small change in the ratio m^0/M_A^0 will shift the nuclear resonance frequency considerably. Further, since m^0 is temperature dependent while M_A^0 is assumed constant, as the temperature is lowered m^0 increases and the frequency for resonance is pulled downward. Also, as the externally applied field increases above H_D, the enhancement factor decreases and therefore the amount of frequency pulling decreases. In Fig. 1(a) the resonance frequency is plotted against the applied field at $T = 1.5$ °K, while Fig. 1(b) is at $T = 4.2$ °K. There appears to be very little frequency pulling at 4.2 °K due to the relatively large anisotropy field, $H_K \simeq 1.0$ kOe. As seen in Fig. 1(a), frequency pulling is observable in manganese ferrite, but is not so strong as to make pulse techniques difficult.[9]

For nuclei in domain walls the enhancement factor is typically an order of magnitude larger than for nuclei within the domains. Thus as long as there is a significant fraction of resonant nuclei in domain walls these nuclei will dominate the resonance behavior. The magnetization of the crystal used here reaches 95% of its saturation value in an external field of about 3 kOe. The externally applied field and the internal demagnetizing field will combine in such a way as to leave the resonance signal due to nuclei within domains unshifted in frequency and undiminished in intensity with increasing H_0 until $H_0 > 3$ kOe. For $H_0 > 3$ kOe the sample is essentially a single domain and the nuclei see an effective field of $H_0 - 3$ kOe.

In the absence of an external field the resonance

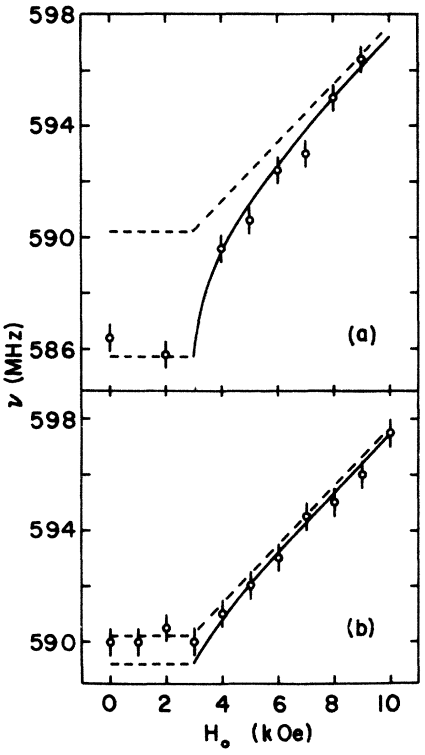

FIG. 1. External field dependence of the resonance frequency of nuclei in domains: Dotted lines are for $\nu = (\frac{1}{2\pi})\gamma_N(H_0 - H_D) + H_N$ while the solid curves are for the frequency pulled case. (a) $T = 1.5\,^\circ$K, $H_K = 0.6$ kOe, $H_N = 559.5$ kOe; (b) $T = 4.2\,^\circ$K, $H_K = 1.0$ kOe, $H_N = 559.5$ kOe.

line consists of two components of roughly the same width, one with a maximum at ~588 MHz, the other with a maximum at ~590 MHz (at 4.2 °K). On increasing the external field from zero, the lower-frequency component decreases in intensity until at $H_0 = 3$ kOe it has essentially vanished, while the higher-frequency component remains unshifted and undiminished until $H_0 = 3$ kOe. Figure 2, which is a plot of echo amplitude versus frequency in an external field of $H_0 = 3$ kOe at $T = 4.2\,^\circ$K, shows that the resonance line is rather well described by a Gaussian curve with half-width at half-maximum of 3.0 MHz (the solid curve in the figure).

III. SUHL-NAKAMURA INTERACTION AND SPIN-SPIN RELAXATION OF FIRST ECHO

In a two-sublattice system the Suhl-Nakamura Hamiltonian is[2]

$$\mathcal{H}_{S\text{-}N} = \tfrac{1}{2}D\left(\sum_j (I_j^z)^2 + \sum_k (I_k^z)^2\right) - \frac{1}{2}\sum_{j\neq j'} B_{jj'}(I_j^+ I_{j'}^- + I_j^- I_{j'}^+)$$

$$-\frac{1}{2}\sum_{k\neq k'} B_{kk'}(I_k^+ I_{k'}^- + I_k^- I_{k'}^+) - \sum_{j,k} C_{jk}(I_j^+ I_k^- + I_j^- I_k^+),$$

where sums over j are over the A sublattice and sums over k are over the B sublattice. This Hamiltonian describes an effective nuclear spin-spin interaction via emission and absorption of virtual spin waves, and is obtained from a second-order perturbation treatment of the hyperfine interaction. In the discussion of transverse relaxation, the first term, which is essentially a self-energy term of quadrupolar nature and cannot contribute to transverse relaxation, can be neglected. The third term is neglected here because it involves only nuclei on the B sublattice, while the last term involves interaction between spins on different sublattices and can be neglected since the second-order nature of the interaction requires energy conservation which is not possible due to the large difference in the hyperfine fields of the two sublattices. Thus, only the second term is retained and the interaction of interest is

$$\mathcal{H}_{S\text{-}N} = -\frac{1}{2}\sum_{j\neq j'} B_{jj'}[I_j^+ I_{j'}^- + I_j^- I_{j'}^+], \tag{3a}$$

with

$$B_{jj'} = A^2 S \frac{1}{N}\sum_{\vec{k}} \frac{1}{\hbar\omega_{\vec{k}}} e^{i\vec{k}\cdot(\vec{r}_j - \vec{r}_{j'})}, \tag{3b}$$

where $A = \hbar\gamma_N H_N/\langle S\rangle$ is the hyperfine constant, $S = \frac{5}{2}$ is the Mn^{2+} ion spin, I_j is the jth manganese nuclear spin, and $\hbar\omega_{\vec{k}}$ is the energy of a spin wave of wave vector $\vec{k}$.

If only spin waves on the A sublattice are considered, the B sublattice will enter only through the exchange constant J and by its effect on the effective anisotropy field $\vec{H}_K = \beta\vec{H}_B + \vec{H}_A$. The ferrimagnetic-spin-wave dispersion relation is then approximately

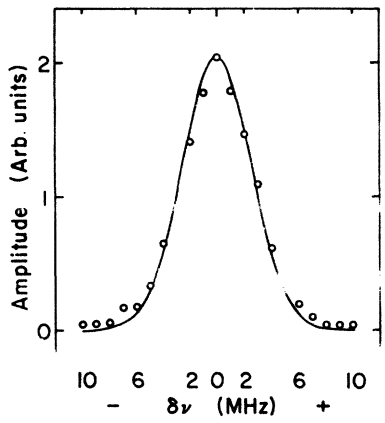

FIG. 2. Frequency dependence of the amplitude of the first echo. $\delta\nu = \nu - \nu_{00}$, where ν_{00} is the frequency at maximum amplitude. The solid curve is a Gaussian with half-width at half-maximum $\delta = 3.0$ MHz. $H_0 = 3.0$ kOe, $T = 4.2\,^\circ$K.

$$\hbar\omega = 2\mu_B(H + H_K) + 2JS_B a^2 k^2 \left(\tfrac{11}{32}\right) , \qquad (4)$$

where ω is the spin-wave frequency, S_B is the B sublattice spin, and $a = 8.5\times10^{-8}$ cm is the lattice spacing.

Mn^{2+} ions on the A sites are surrounded by 12 nearest magnetic neighbors on the B sites, these neighbors can be Mn^{3+}, Fe^{3+}, Fe^{2+}, or Ni^{2+}. On the A sites there are also Fe^{3+} ions, but Mn^{2+} and Fe^{3+} both have spin $\frac{5}{2}$ while the B-site ions have an average spin of 2.385 [since there is a total B-site spin of (9.54/2) per formula unit and there are two B-site ions per formula unit]. From the molecular-field theory of a ferrimagnet,[10]

$$H_{ex}^A = \lambda M_A , \quad H_{ex}^B = \lambda M_B ,$$
$$\lambda = 3k_B T_F / N g^2 \mu_B^2 [S_A(S_A+1)S_B(S_B+1)]^{1/2} , \qquad (5)$$

where T_F is the ferrimagnetic ordering temperature, k_B is Boltzmann's constant, N is the number of ions, μ_B is the Bohr magneton, S_A is the A-site spin, and S_B is the B-site spin. Then,

$$H_{ex}^B = \left(\tfrac{2}{3}\right) S_B \left(\frac{3k_B T_F}{g\mu_B [S_A(S_A+1)S_B(S_B+1)]^{1/2}} \right)$$

since

$$M_B = N_B g \mu_B S_B$$

and

$$N_B = \tfrac{2}{3} N .$$

for $g = 2$ and $T_F = 600\,^\circ$K,

$$H_{ex} = \left(\frac{2 z S_B}{g\mu_B} \right) J \approx 2.6\times10^6 \text{ Oe.}$$

In the long-wavelength approximation the sum over $\vec{k}$ in Eq. (3b) can be replaced by an integral[1,2] which when evaluated yields the asymptotic range function

$$f(r_{jj'}) = \frac{1}{4\pi\alpha} \frac{a_{nn}}{r_{jj'}} \exp\left[-\left(\frac{H + H_K}{\alpha' H_{ex}} \right)^{1/2} \frac{r_{jj'}}{a_{nn}} \right] \qquad (6)$$

and

$$B_{jj'} = \left(\frac{A^2 S}{g\mu_B H_{ex}} \right) f(r_{jj'}) .$$

Here, $a_{nn} = (\sqrt{11}/8)\, a$ is the distance between an A-site ion and its nearest octahedral-site neighbor and $\alpha' = \frac{1}{6}$.

This expression is sufficiently valid in this case[11] since $(H + H_K)/H_{ex} \sim 10^{-2}$ to 10^{-3} for external fields used in this experiment.

Using the results of the calculations of Hone *et al.*[11] the Suhl-Nakamura relaxation rate is

$$\left(\frac{1}{T}\right)_{S\text{-}N} = c\tfrac{1}{6}\pi\sqrt{3}\, g(\omega) \left(\frac{A^2 S}{\hbar g \mu_B H_{ex}} \right)^2 \left(\frac{(\sum_{j'} f_{jj'}^3)^{3/2}}{(\sum_{j'} f_{jj'}^5)^{1/2}} \right)$$
$$\times [\tfrac{1}{3} I(I+1)]^{1/2} [8 - 3/2I(I+1)]^{-1/2} , \qquad (7)$$

where $f_{jj'}$ is the range function (6), the sums are over the A sublattice, $g(\omega)$ is a line-shape function describing the inhomogeneously broadened line, and c is the concentration of Mn^{2+} ions on the A sites.

As discussed by Hone *et al.*,[11] the above expression is a result of the inability of nuclei whose Larmor frequencies differ by more than $B_{jj'}/\hbar$ to interact via the Suhl-Nakamura interaction.

From the form of the asymptotic range function in Eq. (6) the Suhl-Nakamura relaxation rate must decrease for increasing applied field H or for larger values of H_K. Also the relaxation rate is proportional to $g(\omega)$ and therefore must decrease as the frequency is moved off resonance. If the Suhl-Nakamura interaction is responsible for the low-temperature relaxation, the predicted field and frequency dependence should be observed experimentally.

Dipole-dipole interactions will also contribute to the over-all spin-spin relaxation rate. These contributions can be calculated in the usual manner[12] yielding four contributions to the dipolar second moment for manganese on the A sites: (i) interactions with other manganese nuclei on the A sites, (ii) interactions with manganese nuclei on B sites, (iii) and (iv) interactions with Fe^{57} nuclei on the A and B sites. We have

$$M_2^A = [C_{Fe}^A (0.02245)(\tfrac{1}{3})\gamma_{Fe}^2 + C_{Mn}^A (\tfrac{35}{4})\gamma_{Mn}^2]$$
$$\times (\tfrac{3}{4})\gamma_{Mn}^2 \hbar^2 \sum_k^A (1 - 3\cos^2\theta_{jk})^2 / r_{jk}^6$$
$$\text{(sum is over } A \text{ sites)} , \qquad (8a)$$

$$M_2^B = [C_{Fe}^B (0.02245)(\tfrac{1}{3})\gamma_{Fe}^2 + C_{Mn}^B (\tfrac{35}{4})\gamma_{Mn}^2]$$
$$\times (\tfrac{3}{4})\gamma_{Mn}^2 \hbar^2 \sum_l^B (1 - 3\cos^2\theta_{jl})^2 / r_{jl}^6$$
$$\text{(sum is over } B \text{ sites)} . \qquad (8b)$$

Here, $C_N^{A,B}$ is the concentration of nucleus N on the A, B sites, the factor (0.02245) accounts for the natural abundance of Fe^{57}, γ_N is the appropriate nuclear gyromagnetic ratio, r_{jk} is the magnitude of the vector joining nuclei j and k, and θ_{jk} is the angle between the sublattice hyperfine field and the relative position vector r_{jk}. On summing over the lattice out to five lattice spacings the moments are found to be

$$M_2^A = 2.304\times10^7 \text{ sec}^{-2} ,$$
$$M_2^B = 1.689\times10^7 \text{ sec}^{-2} ,$$
$$M_2 = M_2^A + M_2^B = 3.993\times10^7 \text{ sec}^{-2} ,$$

and

$$\Delta = (M_2)^{1/2} = 6.31 \times 10^3 \text{ sec}^{-1} .$$

If the homogeneous line function were Gaussian this would yield a dipole-dipole relaxation time of

$$T_D = 1/\delta = 1/1.178\Delta \approx 134 \ \mu\text{sec} ,$$

where δ is defined as the half-width at half-maximum. This time is nearly an order of magnitude larger than the relaxation times observed at resonance. However, since the homogeneous line profile is expected to be Lorentzian a more correct calculation of the dipole-dipole relaxation time would require determination of the fourth moment, thus[12]

$$1/T_D = \delta = \tfrac{1}{6}\pi\sqrt{3}\,(M_2^2/M_4)^{1/2} M_2^{1/2} ,$$

the ratio $M_4/M_2^2 \approx 3$ for a Gaussian line shape, and as the line profile becomes more nearly Lorentzian this ratio increases, thus, the calculated relaxation time increases.

At 1.5 °K, where the contributions to the observed relaxation rate due to Raman scattering of spin waves and similar processes can likely be safely neglected, there appears to be a frequency-independent relaxation (not directly observed but inferred from the data and discussion of Fig. 5) with a characteristic time of about 600 μsec. If this is assumed to be due to dipole-dipole relaxation, we have the ratio

$$M_4/M_2^2 \sim 9 ,$$

which is not an unreasonable value for a quasi-Lorentzian homogeneous line profile.

The prescription used in the treatment of the Suhl-Nakamura relaxation rate, i.e., Eq. (7), is not applied to the dipole-dipole process since, while the transverse terms in the "secular" dipole-dipole Hamiltonian require mutual spin flips and therefore energy conservation just as the Suhl-Nakamura interaction does, the longitudinal part does not require this and, while being longitudinal in character, is still effective in broadening the homogeneous line. Therefore, since a basic assumption in the above model is that nuclei whose Larmor frequencies differ by more than the characteristic interaction energy[11] cannot interact, the model cannot be applied to the longitudinal part of the dipole-dipole interaction. A more accurate treatment would apply the above prescription to the transverse part and calculate separately the second and fourth moments of the longitudinal portion of the dipole-dipole interaction. However, since in this case the relaxation times due to dipole-dipole effects are very long compared to those due to the S-N interaction, this will not be done here.

Figure 3 shows the frequency dependence of the observed spin echo relaxation time at 4.2 °K (open circles) and at 77.35 °K (solid circles). The solid curves are the frequency dependences of the relaxation times calculated by Eq. (7) assuming a background relaxation time[13] at 4.2 °K of ~155 μsec and of ~17 μsec at 77.35 °K, using a Gaussian line-shape function $g(\omega)$ with half-width at half-maximum of 3 MHz ($\times 2\pi$) in both cases. The data were taken in an external field of 3 kOe, the A-site Mn^{2+} concentration $c = 0.355$: at $T = 4.2$ °K, $H_K = 1.0$ kOe and $H_N = 559.5$ kOe from Fig. 1(b); at 77.35 °K, $H_N = 555.4$ kOe and $H_K = 1.5$ kOe. The exchange field $H_{ex} = 3.75 \times 10^6$ Oe was adjusted to provide the best over-all agreement between calculation and experiment and, while the value used is ~37% higher than that calculated for $T_F = 600$ °K by simple molecular-field theory, represents a not unreasonable value since molecular-field theory is expected to yield a value 30–40% low in the best of cases.[10]

At 4.2 °K the experimental values for the relaxation time follow the predicted field dependence quite well until at lower frequencies (> 3 MHz below resonance) the observed relaxation times are shorter than those calculated. This is due to the asymmetry of the actual inhomogeneously broadened line. For example, spin echoes can be observed continuously from the B-site Mn^{3+} resonance[7] at ~400 MHz up to the A-site resonance, but they vanish for frequencies greater than about 610 MHz.

It is interesting to note that the Suhl-Nakamura relaxation is still visible at 77 °K, as shown by the slight dip in the lower relaxation-time-versus-

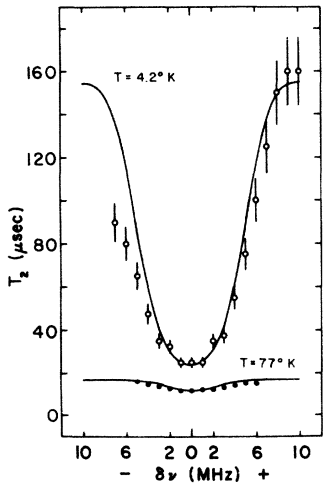

FIG. 3. Frequency dependence of the relaxation time of the first echo in an external field of 3 kOe at 4.2 °K (open circles) and at 77 °K (solid circles). The solid curves are calculated assuming a frequency- and field-independent background relaxation time of 155 μsec at 4.2 °K and at 17 μsec at 77 °K. $\delta\nu = \nu - \nu_{00}$.

frequency curve of Fig. 3. Also, the background relaxation time is strongly temperature dependent suggesting a spin-wave scattering process.

Figures 4(a) and 4(b) show the observed and calculated field dependence of the relaxation time at 1.5 and 4.2 °K, respectively. At $T = 1.5$ °K, $H_N = 559.5$ kOe and $H_K = 0.6$ kOe and the background relaxation time[13] has increased to ~600 μsec.

The frequency dependence of the relaxation time at 1.5 °K is shown in Fig. 5 for the first (open circles) and second (solid circles) echoes. The solid curve for the second echo calculation will be discussed in Sec. IV.

The actual echo amplitudes can be conveniently calculated using the density matrix formalism.[14] At a time $t = 0$, in the absence of external rf fields, the density matrix in the laboratory frame is, in the high-temperature approximation,

$$\rho_1' \propto \exp(\hbar \mathcal{H}_0/k_B T) \simeq 1 + \hbar \mathcal{H}_0/k_B T ,$$

where $\mathcal{H}_0 = \mathcal{H}_Z + \mathcal{H}'$. $\mathcal{H}_Z$ is the Zeeman term and $\mathcal{H}'$ includes the terms responsible for the relaxation, i.e., the dipole-dipole and Suhl-Nakamura terms, and the quadrupole term.

The quadrupole term will be neglected here because of the tetrahedral symmetry of the A sites. Further, the dipole-dipole and Suhl-Nakamura interactions are assumed to be small compared to $\mathcal{H}_Z$ and their primary effect will be to relax the net magnetization towards its equilibrium value and hence broaden the resonance line. Thus, at $t = 0$, in equilibrium

$$\rho_1' = \hbar \omega_0 I_Z ,$$

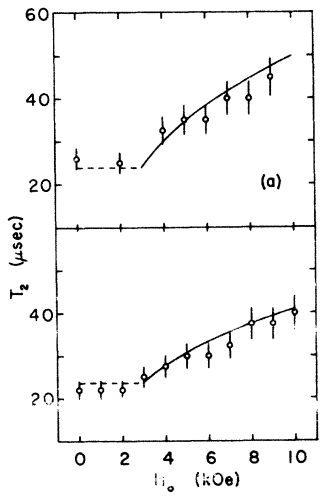

FIG. 4. External field dependence of the relaxation time at resonance of the first echo. (a) $T = 1.5$°K. (b) $T = 4.2$°K. The solid curve in each section is the calculated field dependence.

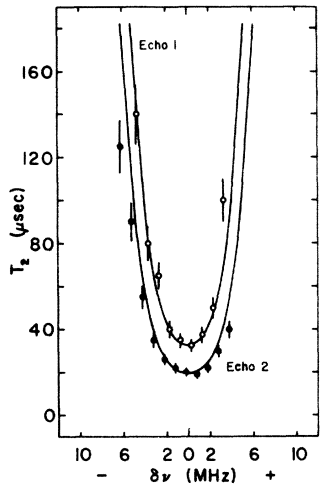

FIG. 5. Frequency dependence of the relaxation time in an external field of 4 kOe of the first echo (open circles) and of the second echo (solid circles) at $T = 1.5$°K. The solid curves are the calculated frequency dependences assuming a background relaxation time of 600 μsec for the first echo. $\delta\nu = \nu - \nu_{00}$.

where ω_0 is the Larmor frequency, is that part of the density matrix describing the nuclear magnetization. In the frame rotating at frequency ω

$$\rho_1 = \hbar \Delta\omega I_Z , \quad \Delta\omega = \omega_0 - \omega .$$

At $t = 0^+$ an rf pulse is applied along the y axis in the rotating frame, then,

$$\rho_2 = U_1 \rho_1 U_1^{-1} ,$$

$$U_1 = \exp[-i(\Delta\omega I_Z + \omega_1 I_y) t_{w_1}] ,$$

where $\mathcal{H}'$ is neglected during the pulse; t_{w_1} is the width of the pulse and $\omega_1/\gamma = H_1$ is the rf pulse strength. If $|\Delta\omega| \ll \omega_1$ the operator U_1 is simply a rotation through angle $\omega_1 t_{w_1}$ about the y axis and can be readily evaluated.[15]

At a time τ after application of the first pulse the density matrix is

$$\rho_3(\tau) = U_2(\tau - t_{w_1}) \times [U_1(t_{w_1})\, \rho_1 U_1^{-1}(t_{w_1})]\, U_2^{-1}(\tau - t_{w_1}) .$$

Here

$$U_2(\tau - t_{w_1}) = \exp[-i\mathcal{H}_2(\tau - t_{w_1})]$$

is the time development operator following the first pulse, which should include the effects of the Suhl-Nakamura interaction on the transverse nuclear magnetization.

The form of $\mathcal{H}_{S\text{-}N}$ [Eq. (3)] makes it difficult to include explicitly in the expressions for the time development operators. However, the previous discussion has shown that the primary effect of $\mathcal{H}_{S\text{-}N}$ is to cause a transverse relaxation which is

described by the relaxation time $(T_2)_{S-N}$; similarly, the dipole-dipole interaction causes relaxation characterized by T_D. Describing all the relaxation processes by a total relaxation time T_2 we find for the transverse magnetization in the rotating frame following a single rf pulse, at a time t,

$$S^*_{(3)}(t) = C_n e^{-t/T_2} \mathrm{Tr}(I^+\rho_3) ,$$

where C_n is a normalization constant.

$\mathcal{H}_2$, the Hamiltonian following the first pulse, contains the Zeeman term as well as the terms causing relaxation. If the major effect of $\mathcal{H}_{S-N}$ and $\mathcal{H}_{d-d}$ are to cause relaxation as described above, we may neglect them[16] in the expression for the time development operator and

$$U_2 = \exp[-i\Delta\omega(t - t_{w_1}) I_Z]$$
$$= \exp(-ia_3 I_Z) .$$

This allows the straightforward computation of $\mathrm{Tr}(I^+\rho_3)$, which in this case is

$$\mathrm{Tr}(I^+\rho_3) = e^{ia_3} \mathrm{Tr}(I^+\rho_2)$$

and

$$\mathrm{Tr}(I^+\rho_2) = \sum_i \sum_j \sum_k I^+_{ij} (U_1)_{jk} (\rho_1)_{kk} (U_1)^*_{ik} .$$

Averaging over the inhomogeneous distribution $g(\omega)$ with the center at ω_{00} and transforming back to the laboratory frame, the observed signal will be proportional to

$$S_{(3)}(t) \simeq \{\exp[i\omega_{00}(t - t_{w_1})]\} G(t - t_{w_1})$$
$$\times \mathrm{Tr}(I^+\rho_2) \exp(-t/T_2) C'_n , \qquad (9)$$

where

$$G(t - t_{w_1}) = \int_{-\infty}^{\infty} d\omega' \exp[i\omega'(t - t_{w_1})] \; g(\omega_{00} + \omega') .$$

If $g(\omega)$ is Gaussian, then $G(t - t_{w_1})$ will be Gaussian with a maximum at $t = t_{w_1}$. This is of course the free induction decay.

During the second pulse, of strength ω_2/γ and length t_{w_2},

$$U_3 = \exp(-i\omega_2 t_{w_2} I_y)$$

and

$$(\rho_4)_{ij} = (U_3\rho_3 U_3^{-1})_{ij} = \sum_k \sum_l (U_3)_{ik} (U_3)^*_{jl} \; (\rho_2)_{kl} e^{(k-l)ia_3} ,$$

$$\mathrm{Tr}(I^+\rho_4) = \sum_n \sum_i (I^+)_{ni} (\rho_4)_{in}$$
$$= \sum_{r=0}^{2I} M_r^{(3)} e^{ria_3} \qquad (r = k - l),$$

$$M_r^{(3)} = \sum_{i=1}^{2I} \sigma_i \sum_k{}' (U_3)_{i+1,k}$$
$$\times (U_3)^*_{l,k-r} (\rho_2)_{k,k-r} ,$$

where $\sigma_i = (I^+)_{i,i+1}$ and $\sum'_k$ is the sum over k such that $k - r \geq 1$, $k \leq 6$.

Following the second pulse

$$U_4 = \exp[-i\Delta\omega I_Z(t - \tau_1 - t_{w_2})] = \exp(-ia_5 I_Z)$$

and

$$\rho_5 = U_4\rho_4 U_4^{-1} .$$

Then,

$$\mathrm{Tr}(I^+\rho_5) = e^{ia_5} \mathrm{Tr}(I^+\rho_4) ,$$

and the signal, after two pulses separated by a time τ, is proportional to

$$S_{(5)}(t) = C''_n \sum_{r=0}^{2I} e^{i\omega_{00}(a_5 + ra_3)} \; M_r^{(3)} G\left(\frac{a_5 + ra_3}{\Delta\omega}\right) e^{-t/T_2} . \qquad (10)$$

From the symmetry of the operators describing the time development during the two pulses (i.e., assumption of pure rotations), the coefficients $M_r^{(3)}$ and therefore the observed signal will be nonzero only for

$$t = \tau_1 + t_{w_2}$$

and

$$t = 2\tau_1 + t_{w_2} - t_{w_1} .$$

These of course are the free induction and first echo, respectively. For more general two pulse excitation conditions, or inclusion of quadrupole terms, etc., as many as $2I$ echoes can be observed, where I is the nuclear spin.

To complete the discussion of the first echo amplitude, the field dependence of the enhancement factor must be included since the observed signal should be proportional to η^2.[17]

Figure 6(a) is a plot of log of echo amplitude at $t = 0$ versus log of $H' = (H_0 - H_D) + (H_K + \alpha m_0)/0.9$. The calculated curve is naturally a straight line of slope $m = -2$. The triangles are the points at 4.2 °K, while the circles are for 1.5 °K.

The preceding discussion of the first echo amplitude is essential to the calculation of the second and third echo relaxation times in Sec. IV.

IV. MULTIPLE ECHOES

Multiple spin echoes have been frequently observed, and various explanations have been applied to the different cases.[14,18-20] For nuclei with $I > \frac{1}{2}$ quadrupole effects can cause as many as $2I$ echoes following a two pulse excitation.[14,18,19] Also, external processes[20] requiring the active participation of the resonant cavity can cause a refocusing of the spin and, consequently, multiple echoes.

The formation of multiple echoes in the present case can be easily visualized if one considers the

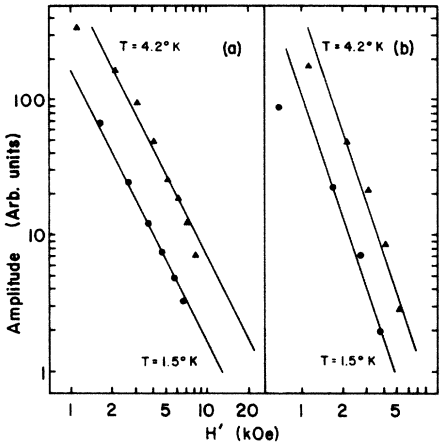

FIG. 6. Field dependence of echo amplitudes. Triangles are at $T = 4.2\,^{\circ}\mathrm{K}$ and circles are at $T = 1.5\,^{\circ}\mathrm{K}$. $H' = (H_0 - H_D) + (H_K + \alpha m_0)/0.9$. (a) First echo, the solid curves are amplitude proportional to $(1/H')^2$, (b) second echo, the solid curves are amplitude proportional to $(1/H')^3$.

reaction of a single spin j' to the partial polarization of the rest of the spin system. During the formation of the first echo, spin j' will feel the net nuclear magnetization in the rotating frame. Since this magnetization represents an internal field in the rotating frame, nucleus j' will respond to this field produced by the echo in much the same way that it would respond to the application of an rf pulse along the direction of echo formation. The reaction of the total spin system will be to refocus again at a time $\Delta t \approx \tau$ after the first echo. This process then continues with ever decreasing amplitude. What is necessary in this process is an interaction between nuclei of sufficient strength to allow repetitive refocusing. The dipole-dipole interaction is too weak, but the long-range nature of the Suhl-Nakamura interaction makes it sufficient for multiple echo formation when there is a large abundance of identical spins. It is expected that the higher numbered echoes will decrease more rapidly with increasing field and pulse separation time τ than do the echoes occurring earlier. For example, since the first echo's amplitude varies as η^2, the second echo's amplitude should be proportional to η^3.

From Eqs. (3) and (6) the Suhl-Nakamura Hamiltonian for spin j' can be written

$$\mathcal{H}_{S\text{-}N}^{j'} = -\frac{1}{2}\left(\frac{A^2 S}{g\mu_B H_{ex}}\right)\sum_{j\neq j'} f(r_{jj'})(I_j^+ I_{j'}^- + I_j^- I_{j'}^+)$$

$$= -\frac{1}{2}\left(\frac{A^2 S}{g\mu_B H_{ex}}\right)\left[\left(\sum_{j\neq j'} f(r_{jj'}) I_j^+\right) I_{j'}^- + \left(\sum_{j\neq j'} f(r_{jj'}) I_j^-\right) I_{j'}^+\right].$$

In equilibrium, $\sum_{j\neq j'} f(r_{jj'}) I_j^{\pm} = 0$. Following the application of a $\frac{1}{2}\pi$ pulse and a π pulse a time τ_1 later, both along the y axis, the magnetization in the x-y plane is no longer zero and, therefore, the sums above do not vanish and there will be an interaction between the nuclear spins. At a time $t = 2\tau_1 + t_{\omega 2} - t_{w_1}$ the components of spin in the x-y plane will refocus along the x axis. At this time, neglecting relaxation for the moment,

$$I_j^+ = I_j^x = I_j^- ,$$

and

$$\mathcal{H}_{S\text{-}N}^{j'} \sim -C_{S\text{-}N}\left(\sum_{j\neq j'} f(r_{jj'}) I_j^x\right)(I_{j'}^- + I_{j'}^+)$$

$$= -C_{S\text{-}N}\left(\sum_{j\neq j'} f(r_{jj'}) I_j^x\right) I_{j'}^x \sim -\omega'_{S\text{-}N} I_{j'}^x . \qquad (11)$$

In general, if $g_e(t)$ is the function describing the x component of nuclear magnetization,

$$\mathcal{H}_{S\text{-}N}^{j'} \sim -\omega_{S\text{-}N} I_{j'}^x g_e(t) .$$

The time development operator following the second pulse is

$$U_4 = \exp[-i\Delta\omega I_Z(t - \tau_1 - t_{w_2}) - i\omega_{S\text{-}N} g_e(t) I_{j'}^x] .$$

$g_e(t)$ is a maximum at $t = 2\tau_1 + t_{w_2} - t_{w_1}$, and at $t = \tau_1 + t_{w_2}$ (i.e., the free induction decay). Thus on the refocusing of the first echo, the spin system sees an effective pulse along the x axis. This pulse is due to the Suhl-Nakamura interaction and causes the formation of the second spin echo, and is partly responsible for the third echo.

The strength of this pulse can be readily estimated since

$$\Delta E_{S\text{-}N}\, T_{S\text{-}N} \sim \hbar$$

or

$$\omega_{S\text{-}N}\, T_{S\text{-}N} \sim 1, \quad \omega_{S\text{-}N} \sim (1/T_{S\text{-}N}) ,$$

while the function $g_e(t)$ will be approximated by a square pulse of width δ_e and height h proportional to the echo amplitude, centered at $t = 2\tau_1 + t_{w_1} - t_{w_2}$, where δ_e is the full width at half-maximum of the first echo.

At $T = 4.2\,^{\circ}\mathrm{K}$, $T_{S\text{-}N} \approx 25\ \mu\mathrm{sec}$, thus,

$$\omega_{S\text{-}N} \sim 4\times 10^4\ \mathrm{sec}^{-1}$$

while

$$\delta_e \sim 5.7\times 10^{-7}\ \mathrm{sec};$$

then

$$\omega_{S\text{-}N}\,\delta_e h \sim 2.3h\times 10^{-2} \sim 0.014\pi h .$$

The constant h is determined by the strength of the first echo in zero field. The rf field felt by the spin system is

$$(\omega_{S-N}/\gamma_{Mn})\eta(H) = (1/\gamma_{Mn})(0.014\pi h)\eta(H) \ . \qquad (12)$$

The calculated properties of the second and third echoes, i.e., field and frequency dependence of echo amplitudes and relaxation times, show virtually no change when h is varied from 0.05 to 0.5. The absolute amplitudes of the second and third echoes will of course depend on the value of h.

Continuing the discussion of Sec. II by treating the first echo as an rf pulse ignoring $\Delta\omega$ during the first echo,

$$U_5 = D_x(-\tfrac{1}{2}\pi)\exp(-i\omega_e t_{w/e} I_y')D_x(\tfrac{1}{2}\pi)$$
$$= D_x(-\tfrac{1}{2}\pi)\Theta D_x(\tfrac{1}{2}\pi)$$

represents a rotation through an angle $\omega_e t_{w_e}$ about the x axis, where the $D_x(\pm\frac{1}{2}\pi)$ are rotations of $\pm\frac{1}{2}\pi$ about the z axis. The density matrix during this pulse is

$$\rho_6 = U_5\rho_5 U_5^{-1},$$

with

$$(U_5)_{jk} = e^{i(k-j)}\Theta_{jk} \ .$$

Further,

$$\mathrm{Tr}(I^+\rho_6) = \sum_{r=-2I}^{2I}\sum_{s=-2I}^{2I} M_{r,s}^{(4)} e^{sia_5} e^{ria_3} \ , \qquad (13)$$

where

$$M_{+|r|,s}^{(4)} = \sum_{p=1}^{(2I+1)-|r|} \delta_{p,p+|r|} \times \sum_l (U_3)_{p+|r|,l+s}(U_3)^*_{p,l}(\rho_2)_{l+s,l} \qquad (14)$$

and

$$M_{-|r|,s}^{(4)} = \sum_{p=1}^{(2I+1)-|r|} \delta_{p+|r|,p} \times \sum_l (U_3)_{p,l+s} \times (U_3)^*_{p+|r|,l}(\rho_2)_{l+s,l}$$

with

$$\delta_{ij} = \sum_{k=1}^{2I} \sigma_k \Theta_{k+1,j}\Theta^*_{k,i} \ ,$$

where, as before,

$$\sigma_k = (I^+)_{k,k+1} \ .$$

Following the first echo, at time t, with $\tau_2 = \tau_1 + t_{w_2} - t_{w_1} - \frac{1}{2}t_{w_e}$,

$$U_6 = \exp[-i\Delta\omega(t-\tau_1-\tau_2-t_{w_e})I_Z] = e^{-ia_7 I_Z} \ ,$$

$$\mathrm{Tr}(I^+\rho_7) = e^{ia_7}\mathrm{Tr}(I^+\rho_6) \ ,$$

and finally, the observed signal will be proportional to

$$S^{(7)}(t) = C_h^m \sum_{r=-2I}^{2I}\sum_{s=-2I}^{2I} M_{r,s}^{(4)} e^{i\omega_{00}(a_7+sa_5+ra_3)} \times G\left(\frac{a_7+ra_3+sa_5}{\Delta\omega}\right) e^{-t/T_2}[\eta(H_0)]^2 \ . \qquad (15)$$

This result also holds for a third external pulse applied at time τ_2 after the second pulse.

Here again, from the assumption of purely rotational pulses, the $M_{r,s}^{(4)}$ are nonzero only at times

$$t = 2\tau_1 + \tau_2 - t_{w_1} + t_{w_e} \ ,$$
$$t = 2\tau_1 + 2\tau_2 - t_{w_2} - t_{w_1} + t_{w_e} \ .$$

Using the value $h = 0.1$ in Eq. (12) the relaxation time of the second echo as a function of frequency was calculated at 1.5 °K, and is shown as the lower solid curve in Fig. 5. To obtain this curve the relaxation time frequency dependence of the first echo, calculated earlier and plotted as the upper solid curve in Fig. 5, was used. The solid circles in Fig. 5 are the measured values of the second echo relaxation time.

The calculated field dependence of the second echo amplitude is compared to the experimental amplitudes in Fig. 6(b). The triangles are for $T = 4.2$ °K and the circles are for 1.5 °K. The calculated lines have the expected $(1/H')^3$ dependence.

Last, the field dependences of the second and third echo relaxation times are shown in Figs. 7 and 8, respectively. The solid curve of Fig. 7(a) is the calculated relaxation time at 1.5 °K, while that of Fig. 7(b) is at 4.2 °K. The open circles are, of course, the measured values. Similarly, the solid curve of Fig. 8(a) is at 1.5 °K and that of Fig. 8(b) is at 4.2 °K.

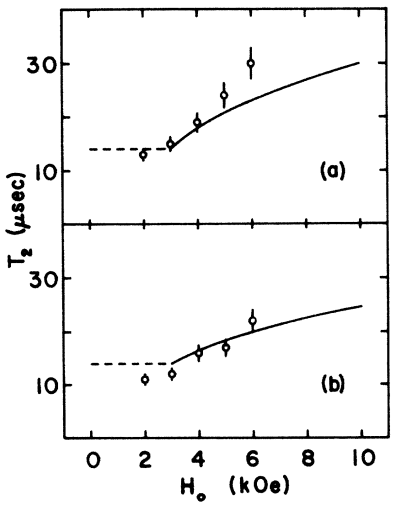

FIG. 7. External field dependence of the relaxation time at resonance of the second echo. The solid curve in each section is the calculated field dependence. (a) $T = 1.5$ °K. (b) $T = 4.2$ °K.

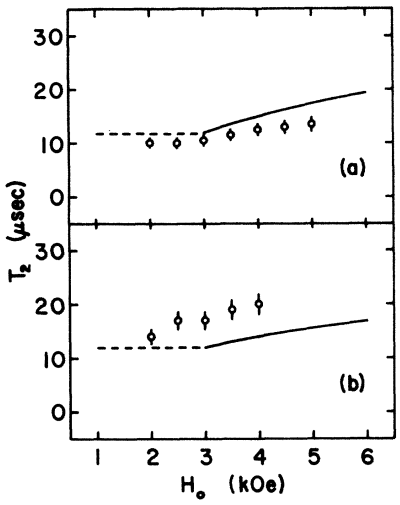

FIG. 8. External field dependence of the relaxation time at resonance of the third echo. The solid curve in each section is the calculated field dependence. (a) $T = 1.5$ °K. (b) $T = 4.2$ °K.

The calculations for the third echo are not expected to be quite correct since the first echo is only partially responsible for the formation of the third echo. By extending the treatment to include the refocusing effects of the second echo, all contributions to the third echo would be accounted for, and a fourth echo would appear. By a natural extension even as many as 22 echoes[4] would be expected. However, it is believed that the agreement between experiment and the calculations outlined above is sufficient to explain the phenomena. The departure of the observed second echo relaxation time for higher fields from the calculated curve, shown in Fig. 7(a), is the most disturbing disagreement. The presence of small quadrupole effects or the departure of the first echo from the purely rotational character assumed for it, are among the possible explanations for this discrepancy.

V. CONCLUSION

The preceding discussion has demonstrated that the Suhl-Nakamura interaction is responsible for the low-temperature spin-spin relaxation and for the formation of multiple echoes in manganese ferrites. These two phenomena, having the same origin, should occur together in other materials. Where the Suhl-Nakamura interaction is known to be strong both relaxation and multiple echo formation should occur.

A material with simpler crystal and magnetic structures exhibiting both of these effects would provide a better opportunity for comparison between experiment and theory. However, in many of the materials in which the Suhl-Nakamura interaction exists and has been studied (e.g., MnF_2, $KMnF_3$, etc.), frequency pulling is so strong that pulse techniques become difficult and spin echoes, if any are observed, have small amplitudes, and multiple echoes are probably unobservable. There are, however, other materials, such as cobalt powder, which exhibit both multiple echoes and Suhl-Nakamura relaxation. In cobalt, however, the quadrupole interaction also contributes to the formation of the first seven echoes and therefore complicates the analysis. EuO and EuS are magnetic insulators with the NaCl structure and seem well suited for an analysis such as is given here. Also, the relaxation time measurements reported by Raj *et al.*[21] suggest that the Suhl-Nakamura interaction is responsible for the low-temperature relaxation. Thus a field dependence study of these crystals would be of considerable interest.

ACKNOWLEDGMENTS

We are indebted to Professor R. Poplowsky of the University of Toledo who supplied the crystal on which these measurements were made. This work was supported by the National Research Council of Canada.

[1]H. Suhl, Phys. Rev. 109, 606 (1958); J. Phys. Radium 20, 333 (1959).
[2]T. Nakamura, Prog. Theor. Phys. 20, 547 (1958).
[3]A. J. Heeger and T. W. Houston, Phys. Rev. 135, A661 (1964).
[4]C. W. Searle, J. Davis, A. Hirai, and K. Fukuda, Phys. Rev. Lett. 27, 1380 (1971).
[5]M. P. Petrov and A. A. Petrov, Izv. Akad. Nauk SSSR Ser. Fiz. 34, 1003 (1970) [Bull. Acad. Sci. USSR Phys. Ser. 34, 894 (1970)].
[6]F. W. Harison, W. P. Osmond, and R. W. Teale, Phys. Rev. 106, 865 (1957); see also T. Kubo, A. Hirai, and H. Abe, J. Phys. Soc. Jap. 26, 1094 (1969).
[7]T. Kubo, A. Hirai, and H. Abe, J. Phys. Soc. Jap. 26, 1094 (1969).
[8]H. Yasuoka, J. Phys. Soc. Jap. 19, 1182 (1964).
[9]P. G. de Gennes, P. A. Pincus, F. Hartmann-Boutron, and J. M. Winter, Phys. Rev. 129, 1105 (1963).
[10]J. S. Smart, *Effective Field Theories of Magnetism* (Saunders, Philadelphia, Pa., 1966), Chaps. 4 and 12.
[11]D. Hone, V. Jaccarino, T. Ngwe, and P. Pincus, Phys. Rev. 186, 291 (1969).
[12]J. H. Van Vleck, Phys. Rev. 74, 1168 (1948); A. Abragam, *Principles of Nuclear Magnetism* (Oxford U. P. New York, 1961), Chap. IV.
[13]The background relaxation times at the three temperatures were chosen to provide the best fit to the observed data. The processes responsible are assumed to the

frequency and field independent as expected of dipole-dipole and Raman scattering relaxation processes.
[14]The procedure and notation used is similar to that of H. Abe, H. Yasuoka, and A. Hirai, J. Phys. Soc. Jap. 21, 77 (1966).
[15]A. R. Edmunds, Angular *Momentum in Quantum Mechanics* (Princeton U. P., Princeton, N. J., 1957).
[16]The primary contribution of these terms is already included in Eq. (9).
[17]A. Narath, in *Hyperfine Interactions*, edited by A. J. Freeman and R. B. Frankel (Academic, New York, 1967), Chap. 7, p. 307.
[18]A. Abragam, *Principles of Nuclear Magnetism* (Oxford U. P., New York, 1961), Chap. VII.
[19]I. Solomon, Phys. Rev. 110, 61 (1958).
[20]L. G. Rowan, Phys. Rev. 167, 326 (1968).
[21]K. Raj, T. J. Burch, and J. I. Budnick, Int. J. Magn. 3, 355 (1972).